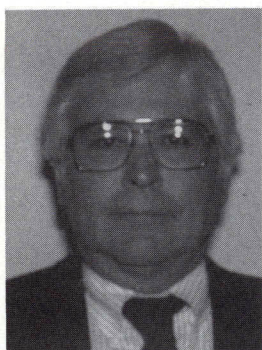


Behavior of Hollow-Core Slabs Subject to Edge Loads



Alex Aswad, Ph.D., P.E.

Associate Professor of Engineering
Penn State University at Harrisburg
Harrisburg, Pennsylvania



Francis J. Jacques, P.E.

President
Jacques & Aswad, Inc.
Denver, Colorado

Presents the results of a comprehensive series of tests on 8 in. (203 mm) thick extruded hollow-core (Dy-Core) slabs. Concentrated loads were applied at the edges of the slabs to produce localized shear or shear-torsion failures. No transverse deck reinforcement was provided. In most cases, the tests were carried through to failure. Based on the test results and a review of existing literature, it is recommended that allowable edge service loads can vary between 3.5 and 3.8 kips (15.6 to 16.9 kN) for the given geometry of the floor system, normal prestress forces and specified concrete strength.

Precast, prestressed concrete hollow-core slabs (Dy-Core), manufactured by an extrusion process, are widely used in North America and throughout the world. Analysis of these units under uniform load is routine and presents no special difficulty. However, in many floor or roof applications, designers encounter the case of having to design for concentrated point loads at the slab edge. Such edge loads are produced whenever steel headers are used to frame around openings and, occasionally, from posts at upper levels of framing.

In general, hollow-core slab sections have good lateral distribution properties. However, elastic plate analysis indicates that transverse bending moments do occur as a result of point loads. The slabs are usually topped with adjacent slabs connected by field-placed grout in keyway joints. This allows the transfer of vertical shear between the units but allows practically zero moment transfer capacity across

the joint. Additionally, significant shear and torsion stresses are also produced near the bearing due to edge loads, especially when loads are located close to the ends.

As a consequence of the zero slump mix used in hollow-core slabs, it is virtually impossible in a normal production run to place any mild steel reinforcement in the precast concrete member transverse to the strand direction or to reinforce the webs. Therefore, without mild steel reinforcement, usual concrete design procedures do not apply and either full-scale testing or complex mathematical models become essential to predict safe maximum permissible edge point loads for a given section.

Under concentrated loads, the voids in hollow-core slabs undergo transverse deformations due to multi-cell deformations similar to a Vierendeel truss (Fig. 1). Although these deformations are small in hollow-core slabs, they do, however, affect the

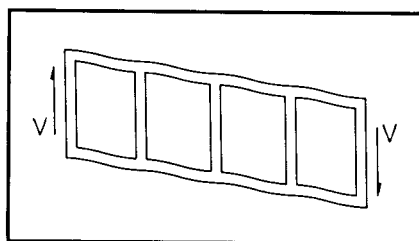


Fig. 1. Cell distortions and shear deformations.

ability of the slabs to transfer loads to adjacent webs and slabs. Prediction of such capacities using finite element analysis methods (FEM) is complex. Thus, full-scale testing appears to be a more desirable alternative.

PREVIOUS RESEARCH AND LITERATURE REVIEW

Several investigations¹⁻¹⁵ have been conducted in the past two decades on hollow-core slabs with grouted or connected joints. Most of these investigations involved load testing while some studies¹⁰⁻¹² included elaborate rational analysis with matrix or finite element methods applied to idealized, uncracked sections. The majority of tested decks included special section geometries, end openings,² midspan cutouts^{3,4} or slabs with variable widths.⁴ These tests primarily focused on lateral load distribution in the presence of point or line loads but did not include testing for limits due to edge loads.

The tests reported herein were designed to examine edge loads controlled by local punching shear failures or a combination shear-torsion failure in the webs of the hollow-core members. A more detailed discussion of previous research on hollow-core slabs is contained in the original Dy-Core report (see Ref. 1).

In studying prior research, the only reports examining the behavior of Dy-Core slabs are by Stanton.^{12,13} Here, tests were conducted on 12 in. (305 mm) thick slabs with the cross section shown in Fig. 2. The tests were done primarily to determine lateral load distribution characteristics of the system. Slab spans were 50 ft (15.2 m) center-to-center of bearing as depicted in Fig. 3. Measurements included both deflections and strains under unit loads.

Stanton developed a finite strip

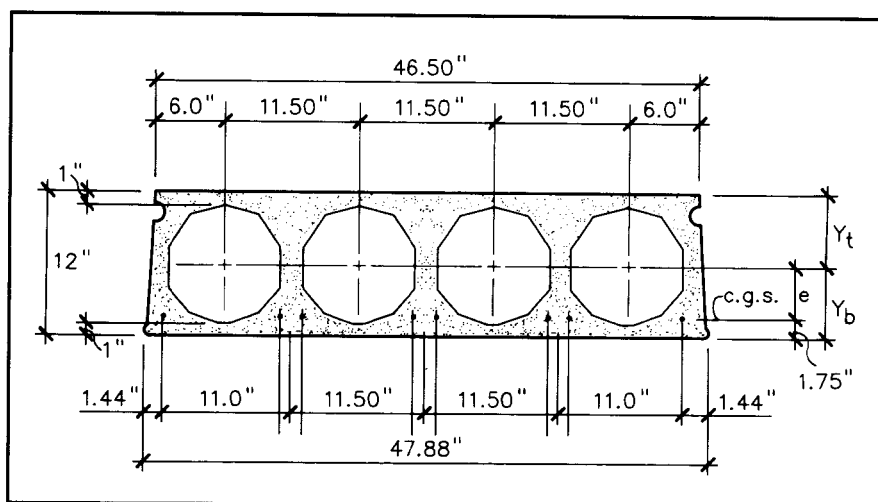


Fig. 2. Cross section of 12 in. (254 mm) deep hollow-core slab.

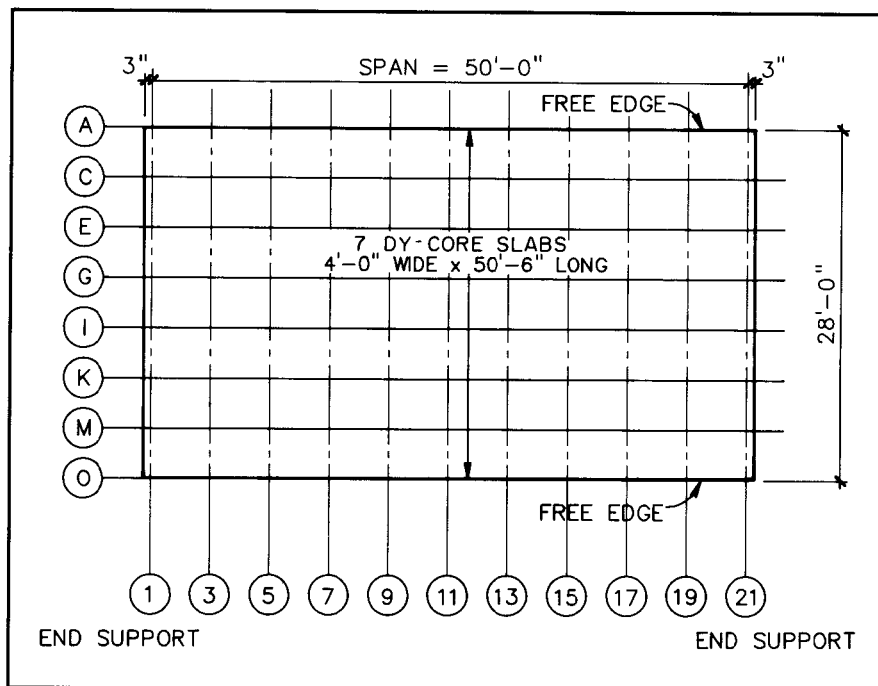


Fig. 3. Plan view of hollow-core slab test deck (see Ref. 13).

method and compared calculated predictions of distribution to the measured "deflection coefficients," defined as the ratio of local deflection divided by the average deflection from all gauges. Two graphs of interest are reproduced as Figs. 4 and 5. Fig. 4 is related to a load applied at mid-width while Fig. 5 addresses the case of an edge load. Good correlation between calculated and measured lateral load distribution was observed under service loads.

Based on full-scale tests on simply supported hollow-core slabs, Venkateswarlu et al.¹⁴ found a satisfactory agreement between the calculated deflections, moments and shears, and the

corresponding experimental values.

The FIP report¹⁵ contains useful information on European practice dealing with allowable edge loads and load distribution for hollow-core slabs. In summary, for edge loads, the FIP report provides the following recommendation for maximum allowable service edge load:

$$F = 7.87 f_c t \quad (1)$$

where

F = allowable service edge load (lbs)

$$f_c = 116 + 0.05 f'_c \text{ (psi)} \quad (2)$$

t = flange thickness (in.)

Eqs. (1) and (2) are based on flexural cracking analysis of the top flange

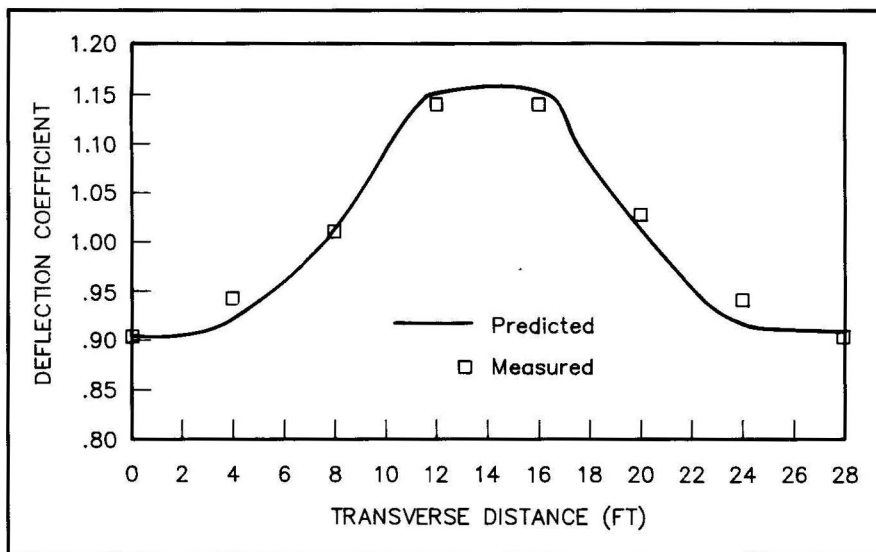


Fig. 4. Deflection profile for load at mid-width (see Ref. 13).

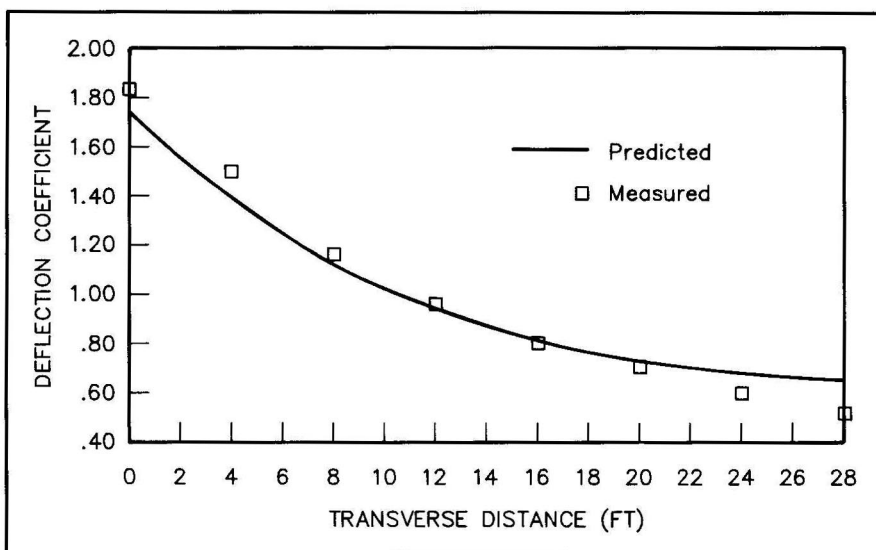


Fig. 5. Deflection profile for load at free edge (see Ref. 13).

under transverse moment. The equations are valid when transverse reinforcement is omitted, provided, of course, permissible values of shear, torsion and punching shear have been checked and are not exceeded.

CODES, STANDARDS AND DESIGN PRACTICE

Many precast concrete producers and design engineers have developed in-house guidelines for distribution widths and have also included recommendations for safe point loads on slab edges. The distribution widths are generally expressed as a fraction of the span, L , and involve defining an estimate for the number of slabs contributing to the floor system. However,

there appears to be no rational analysis or uniform standards developed in the United States that provide authoritative guidance on maximum edge point loads to control punching shear or localized shear-torsion failures.

Regarding distribution widths, in 1985 PCI published the Hollow-Core Design Manual,¹⁶ which contains recommendations for "effective resisting widths" (Fig. 6). These widths vary between $0.5L$ at midspan to 4 ft (1.22 m) near the supports for interior loads (at some distance from the edge). For edge loads, the widths become $0.25L$ at midspan and 1 ft (305 mm) at the supports. The rules apply to hollow-core slab systems in which the effective width of a given system is at least equal to its span length.

Supplementary rules are included for the effect of opening size on effective widths (Fig. 7). This method is generally considered safe if the stated values are used. Recognizing the importance of void geometry, no recommendations on permissible edge loads are included in the Hollow-Core Design Manual. The PCI Design Handbook¹⁷ also contains similar simplified rules on lateral distribution but, again, no guidance on edge loads.

ACI-ASCE Joint Committee 550 is currently preparing a state-of-the-art report on precast concrete structures to serve as a guide for proposed changes to Chapter 16 of ACI 318-95. In its deliberations to date (January 1992), the committee has not offered any new information on the subject of either allowable edge loads or lateral distribution of response to edge loads.

TEST PROGRAM

The entire test program comprised three series of tests, labeled Series I, II and III. Each series of tests is described in the following paragraphs.

Series I Tests

In 1989, a full-scale pilot testing program on hollow-core slabs was conducted at the Finrock Industries, Inc., plant in Orlando, Florida, on 8 in. thick x 4 ft wide (203 mm x 1.22 m) units using the cross section shown in Fig. 8. The 10 tests covered by this program are designated as Series I in this paper. The important results are summarized in Table 1. Sketches of the cracking/failure patterns can be found in Ref. 1.

The tests were conducted on single slabs labeled Slab A and Slab B. Slab A had a center-to-center span of 28 ft 11 in. (8.81 m), except for Test No. 5, which was conducted after one corner was damaged and the span was reduced to 25 ft (7.62 m). Slab B had a center-to-center span of 26 ft 9 in. (8.15 m).

The strand pattern consisted of five $\frac{1}{2}$ in. (12.7 mm) diameter, low-relaxation strands stressed to $0.70 f_{pu}$ and placed in the interior webs. Other than the slab self-weight, there were no other loads imposed except the edge load which was applied through a typ-

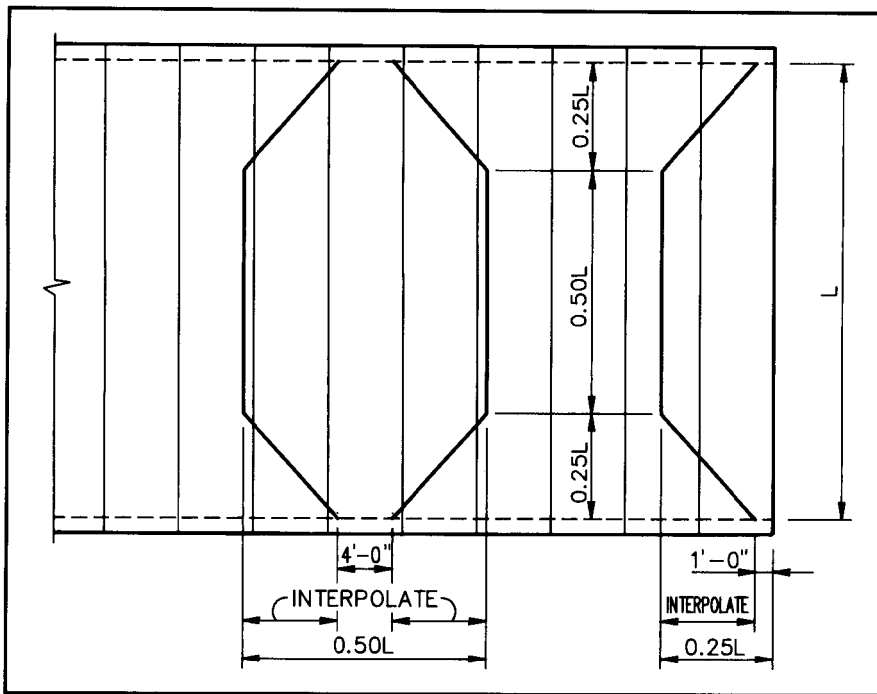


Fig. 6. Effective resisting width of slab for interior and edge locations (see Ref. 16).

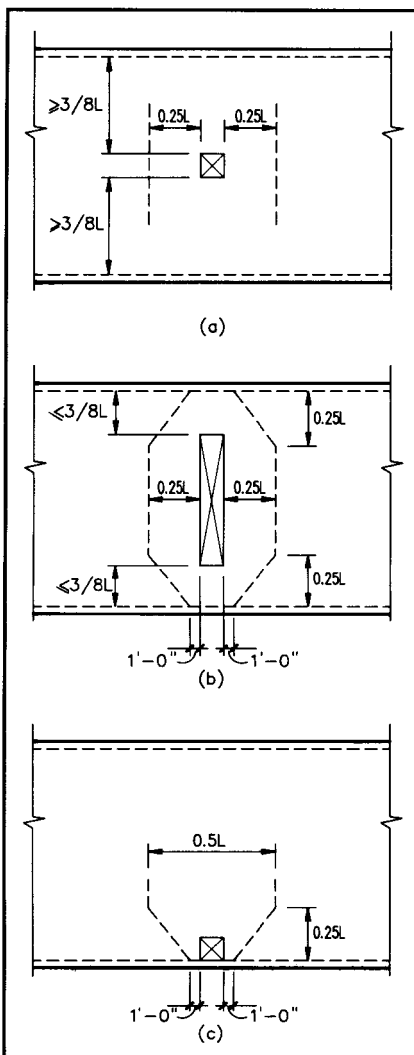


Fig. 7. Effect of openings on effective widths of hollow-core slabs (see Ref. 16).

tions varied between $0.15L$ and $0.5L$.

Table 1 shows the results of this test series. The low failure load obtained in Test No. 4 on Slab A was judged to be partly the result of slab damage at one end from previous tests and from a broken corner that existed at the start of testing. Therefore, it was deemed appropriate to disregard this result.

Test No. 9 on Slab B (point load at $\frac{3}{8}L$) displayed a premature shear-torsion failure at the end nearest the load. It is believed this was partly due to precracking at the end from previous Test No. 7.

Series II Tests

A second full-scale series of tests on 8 in. thick x 4 ft wide (203 mm x 1.22 m) hollow-core slabs was conducted later in the same year. These tests were supervised by the first author. The geometry of the slab cross section was the same as for the earlier tests (see Fig. 8).

Two types of test setups were used: a single and a double-slab layout (see Fig. 9). In the double-slab layout, the shear key between the slabs was

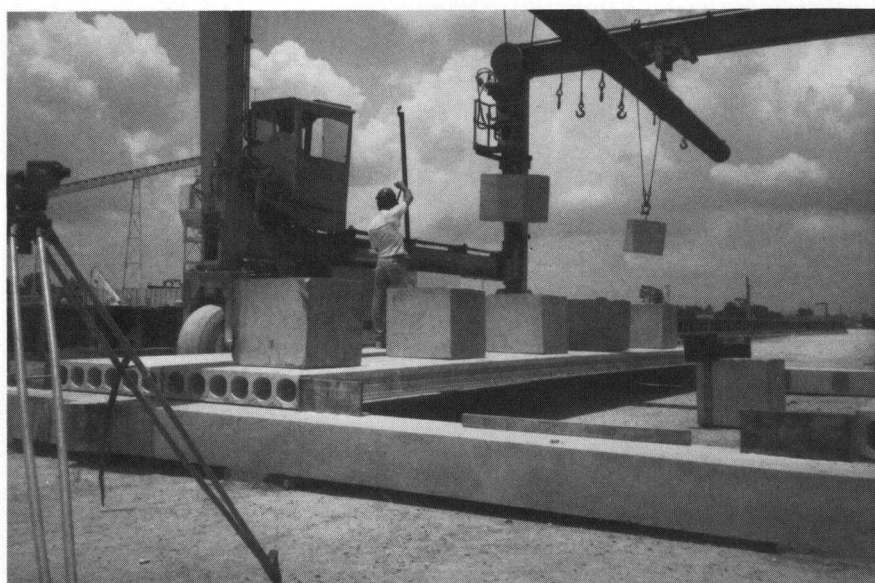
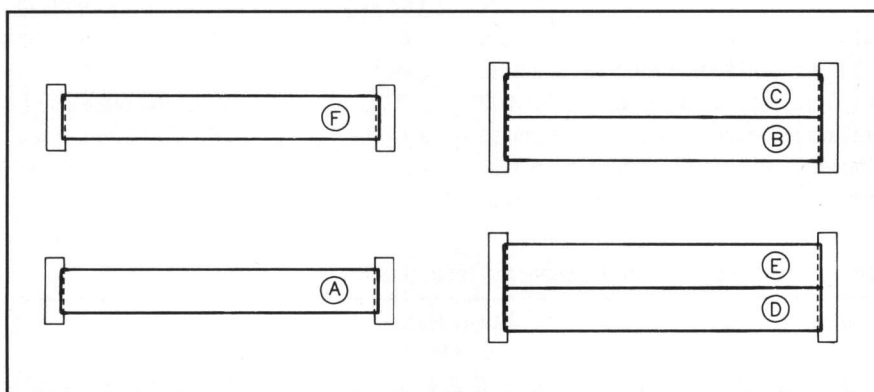
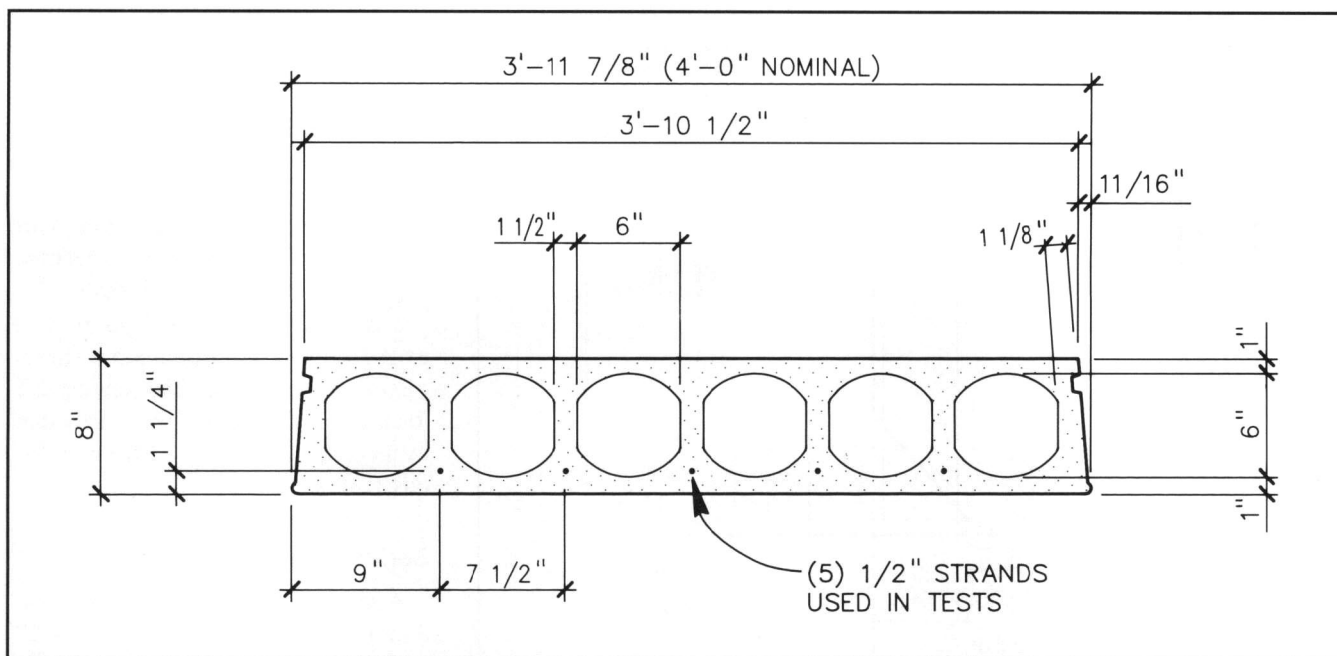
ical 6 in. x 4 in. x $\frac{3}{8}$ in. x 1 ft (152 x 102 x 9.5 x 305 mm) long angle acting on a 6 in. long x 4 in. wide (152 x 102 mm) edge bearing surface. Estimated concrete strength at testing time was 8500 psi (58.6 MPa). Edge load loca-

Table 1. Summary of Series I pilot load tests (Load Q at variable x/L).

Series No.	Test No.	x/L ratio	Failure load, Q (kips)	Type of failure
Slab A load tests				
I	1	0.497	16.2	Full length punching failure in top and bottom flanges
I	2	0.339	12.0	Typical punching shear
I	3	0.147	14.5	End shear-torsion
I	4	0.339	8.7	Early failure due to precracked slab corner at left end
I	5	0.228*	14.5	Shear at end of shortened slab
Slab B load tests				
I	6	0.500	16.1	Typical punching
I	7	0.159	11.1	Shear-torsion at end
I	8	0.159	12.4	Shear-torsion at end
I	9	0.378	13.4	Shear-torsion at end; end region previously cracked by shear-torsion from opposite edge load test
I	10	0.378	13.5	Typical punching shear

Note: 1 kip = 4.45 kN.

* Ratio x/L is short slab.



grouted and cured before the tests started. Six slabs labeled A to F were tested. A center-to-center span, $L = 28$ ft (8.53 m), was used in all the tests. The total slab length was 28 ft 4 in. (8.64 m). An overview of the general experimental setup can be seen in Figs. 10 and 11.

The results of these tests are summarized in Table 2 and are numbered 2 through 14. Results for Tests 1, 6 and 9 are not shown since they were proof tests to calibrate deflection response measurements. The sketches of the various test setups, selected individual test descriptions, critical measured geometric properties and cracking/failure patterns are found in Ref. 1.

The strand pattern consisted of five 1/2 in. (12.7 mm) diameter, low-relaxation strands stressed to $0.70 f_{pu}$ and placed in the interior webs. The stress-strain curve for the strand showed an ultimate tensile strength of $f_{pu} = 281$ ksi (1938 MPa). Concrete strength at time of testing was $f'_c = 8555$ psi (59 MPa).

Several types of superimposed loading patterns were used depending on the test case, all of which are shown in Appendix 2 of Ref. 1. Typical 1.28 kip (5.7 kN) concrete blocks were positioned over slab centerlines at various spacings before applying the edge load. The only exception was Slab F, where no load blocks were used. The

Table 2. Summary of Series II load tests.

Series No.	Test No.	Failure load Q (kips)	Type of failure	Single or double layout; Type of additional load
Load Q at midspan				
II	8	15.8	End shear-torsion (precracked end)	Double slab; light load
II	10	14.0 12.0	No punching Typical punching shear (2 x 8 in. pad size)	Double slab; service load
II	11	14.0 13.5	No punching Typical punching shear (2 x 8 in. pad)	Double slab; service load
II	13	11.5	Typical punching shear (Slab F, $t = 8$ in.)	Single slab; no load
Load Q at 0.33L				
II	2	12.4	Typical punching shear	Single slab; service load
II	3	12.4	Typical punching shear	Single slab; service load
II	4	11.9	Typical punching shear	Single slab; service load
Load Q at 0.25L				
II	7	14.5	Shear-torsion	Double slab; light load (4 x 12 in. pad)
II	7	17.0	No failure	Double slab; light load (4 x 12 in. pad)
II	12	10.0	Shear-torsion (Slab F, $t = 8$ in.)	Single slab; no load
II	14	10.9	Shear-torsion (Slab F, $t = 8$ in.)	Single slab; no load
Load Q at 0.18L				
II	5	12.5	Shear-torsion	Single slab; service load

Note: 1 kip = 4.45 kN.

Table 3. Summary of Series III load tests.

Series No.	Test No.	Failure load Q (kips)	Type of failure	Single or double layout; type of additional load
Load Q at 0.23L to 0.25L				
III	16	15.2	Typical punching shear	Single slab; service load (\pm)
III	17	14.5	Typical punching shear	Single slab; service load (\pm)
Load Q at 0.18L				
III	19	17.5	Typical punching shear	Single slab; service load (\pm)
III	20	14.5	Shear-torsion	Single slab; service load (\pm)

Note: 1 kip = 4.45 kN.

equivalent service load mentioned in the tables corresponds to 54 psf (2.59 kPa). A "light load" is much smaller.

Edge load locations varied between 0.18L and 0.5L and were applied over 4 x 12 in., 3 x 8 in. or 2 x 8 in. (102 x 305 mm, 76 x 203 mm or 51 x 203 mm) bearing pads.

The observed failure mode for a typical punching shear is seen in Fig. 12 and in the sketch of Fig. 13, both for Test No. 13. The observed failure mode for a typical shear-torsion failure is seen in the photograph of Fig. 14 and in the sketch of Fig. 15, both for Test No. 14.

Series III Tests

A third series of tests on single units, labeled Series III, was conducted on Slabs D and E taken from the Series II tests. Loads were applied on the previously untested edges. These tests were performed on August 25 and 26, 1989, and were supervised by Greg Black. This series covered Test Nos. 15 to 20. The results are summarized in Table 3.

The estimated concrete strength at test time was 9200 psi (63.5 MPa). Test No. 15 was a "proof test" with loads of 9 and 10.5 kips (40 and 47 kN) applied at the one-quarter points. The test was not carried to failure. Tests 16 and 17 were failure tests where the edge load was applied at $L/4$. Test 18 had load applied at 0.5L but the available jack stroke was not sufficient to carry the test to failure. In Tests 19 and 20, the load was located at 0.18L from the end. The bearing pad under the edge load was 3 x 8 in. (76 x 203 mm) for the entire series.

DISCUSSION OF RESULTS

Failure Modes

The test results from Series I, II and III are combined in Tables 4 through 7, with each table grouping the results according to the location of the load from the ends:

- Table 4 shows results for edge loads at midspan.
- Table 5 shows results for edge loads at 0.33L to 0.38L.
- Table 6 shows results for edge loads at 0.23L to 0.25L.

Table 4. Edge load Q at midspan.

Series No.	Test No.	Failure load Q (kips)	Adjusted Q value (kips)	Type of failure	Single or double slab layout; type of load
I	1	16.2	14.6	Punching shear, full length	Single slab; no load
I	6	16.1	14.5	Typical punching shear	Single slab; no load
II	8	15.8	14.2	End shear-torsion (precracked end)	Double slab; light load
II	10	14.0 12.0	12.6	No punching Typical punching shear (2 x 8 in.)	Double slab; service load
II	11	14.0 13.5	12.6	No punching Typical punching shear (2 x 8 in. pad)	Double slab; service load
II	13	11.5	11.5	Typical punching shear (Slab F, $t = 8$ in.)	Single slab; no load

Note: 1 kip = 4.45 kN.

Table 5. Edge load Q between $0.33L$ and $0.38L$.

Series No.	Test No.	Failure load Q (kips)	Adjusted Q value (kips)	Type of failure	Single slab layout; additional type of load
I	2	12.0	10.8	Typical punching shear	No load
I	4	[8.7]	Disregard	Premature end shear failure; unit had precracked corner	No load
I	9	13.4	12.1	Premature end shear failure; Test 7 precracked unit	No load
I	10	13.5	12.1	Typical punching shear	No load
II	2	12.4	11.2	Typical punching shear	Service load
II	3	12.4	11.2	Typical punching shear	Service load
II	4	11.9	10.7	Typical punching shear	Service load

Note: 1 kip = 4.45 kN.

- Table 7 shows results for edge loads at $0.15L$ to $0.18L$.

For edge load Q , between $0.33L$ and $0.50L$, Tables 4 and 5 indicate that, unless the slab is precracked by handling or by a previous test, the expected failure can be predicted to be a localized punching shear. As seen in the photographs, this failure often spreads out over a length of 6 ft (1.83 m) or more at the lower flange level.

For a load Q acting at a distance between $0.15L$ and $0.25L$ from the end (Tables 6 and 7), the predominant failure mode is a shear-torsion failure near the end with a diagonal web crack on the outside face. The three

exceptions to this were Tests 16, 17 and 19 from Series III, which failed by punching shear at relatively high load values. These cases do not have an easy explanation.

From actual measurements of the slab cross sections, it was found that increases in flange and area properties over the nominal values were quite common in the production line slabs. It is possible that local flange and web thickness increases near the end may have contributed to an increase in the shear-torsion capacity such that a punching failure was triggered instead.

The shear-torsion failures were characterized by a diagonal crack

which appeared on the vertical edge of the slab and continued in a spiral shape along the top and bottom. Strand slippages were noticed at the end of some tests but were minor.

Examination of the literature shows that hollow-core slabs under concentric loading experience one of three types of non-local failure modes (Fig. 16): shear-compression, shear-tension, or anchorage slippage.

When eccentric or edge loads are applied, then significant local torsion stresses are added, and it appears that the predominant failure pattern is initiated by localized shear-tension cracking at the exterior web followed by a sudden rise in the diagonal tension stresses in adjacent inner webs, which results in a brittle failure. The reason for this sudden worsening of the stress situation and chain reaction is that torsional stresses in a "split" tube (after first cracking) are much higher than in a multi-cell closed tube.

Thus, it is believed that the analysis of shear capacity based on the standard beam approach, which neglects the torsional effects, is not appropriate for hollow-core slabs subject to edge loads.

Adjustment Factors

The major objective of this research program was to develop recommendations for permissible service edge loads for 8 in. thick x 4 ft wide (203 mm x 1.22 m) hollow-core slabs. A total of 28 significant test results were measured for the tested slabs.

The raw data from these tests are listed in Tables 1 through 3 and in the third column of Tables 4, 5, 6 and 7. Prior to using these test values, corrections were applied to normalize the test data to reflect a standard member cross section and a standard concrete strength.

All the slabs, except Slab F in Series II, had a larger overall thickness than the nominal 8 in. (203 mm) thick slab. This resulted in an increase in the flange thickness and also an increase in the height at the potential failure plane. After reviewing the actual section geometries, a correction factor of 0.9 was selected to approximate the ratio of the cross-sectional area of the

Table 6. Edge load Q at $0.23L$ to $0.25L$.

Series No.	Test No.	Failure load Q (kips)	Adjusted Q value (kips)	Type of failure	Single or double slab layout; type of load
I	5	14.5	13.1	Shear-torsion	Single slab; no load
II	7	14.5	13.0	Shear-torsion (pad size: 4 x 12 in.)	Double slab; light load
II	7	17.0	15.3	No failure (pad size: 4 x 12 in.)	Double slab; light load
II	12	10.0	10.0	Shear-torsion (Slab F, $t = 8$ in.)	Single slab; no load
II	14	10.9	10.9	Shear-torsion (Slab F, $t = 8$ in.)	Single slab; no load
III	16	15.2	13.1	Typical punching shear	Single slab; Service load
III	17	14.5	12.5	Typical punching shear	Single slab; Service load

Note: 1 kip = 4.45 kN.

Table 7. Edge load Q at $0.15L$ to $0.18L$.

Series No.	Test No.	Failure load Q (kips)	Adjusted Q value (kips)	Type of failure	Single slab layout; additional type of load
I	3	14.5	13.1	Shear-torsion	No load
I	7	11.1	10.0	Shear-torsion	No load
I	8	12.4	11.2	Shear-torsion	No load
II	5	12.5	11.2	Shear-torsion	Service load
III	19	17.5	15.1	Typical punching shear	Service load
III	20	14.5	12.5	Shear-torsion	Service load

Note: 1 kip = 4.45 kN.

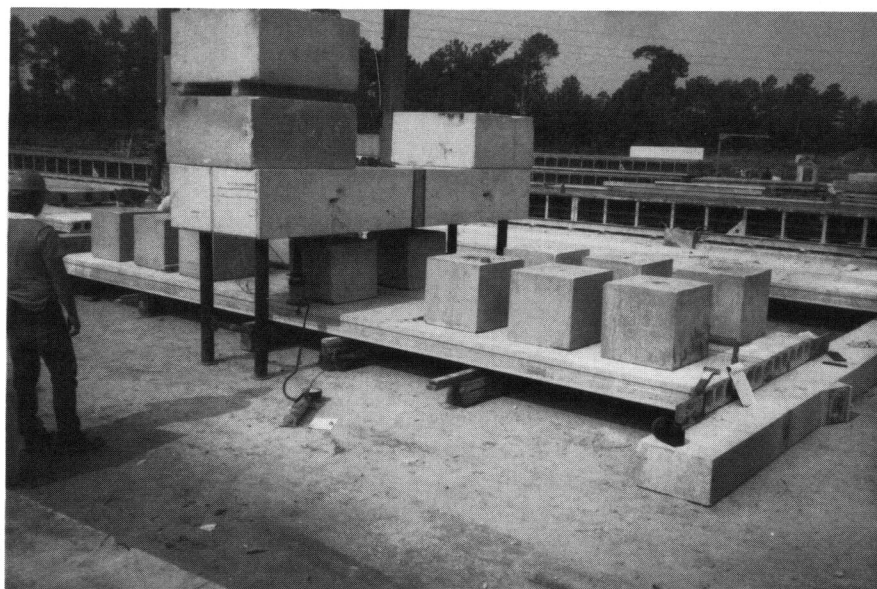


Fig. 11. Test setup showing adjacent slabs, quasi-uniform loading and reaction beam over slabs.

nominal slab to the "as-cast" slab.

To reflect the higher strength concrete at time of the Series III tests, an additional adjustment factor of 0.96 was applied to the test results. This value was derived by assuming that failure values for punching shear and/or end shear capacities are both proportional to $\sqrt{f'_c}$. Thus, we have $\sqrt{8555/9200} = 0.96$.

When examining shear-torsion strengths for loading near the supports, there is a beneficial effect due to lateral load distribution for a multiple slab configuration. Thus, a factor greater than 1.0 could have been applied to the results from the single slab test setup. However, at this stage, it was felt that such an adjustment could lead to unconservative values.

Column 4 of Tables 4 through 7 shows the retabulated results from the three Test Series I, II and III, after adjustments to normalize the test loads. These adjusted loads are then used to determine the final recommendations for allowable edge service loads.

Service Load and Structural Safety

After normalizing the test results, the selection of an appropriate service load was investigated. Without specific guidance from ACI standards or PCI practice, the authors considered the following three approaches from which they selected the lower bound value:

1. Probabilistic Method — The first method follows a probabilistic approach to structural safety which is believed to be rational and current state-of-the-art for concrete design. The test data from all three test series contained in Tables 4 through 7 were first checked to verify that they comply with the usual test for a normal frequency distribution curve. A plot of the test data points and the distribution check calculations are shown in Fig. A1 of Appendix A.

A statistical analysis was then performed showing an average failure load of 12.36 kips (55.0 kN) with a standard deviation of 1.53 kips (6.8 kN). See Table A1 in Appendix A.

The calculation of allowable service load was then arrived at by following



Fig. 12. Midspan failure (Test No. 13).

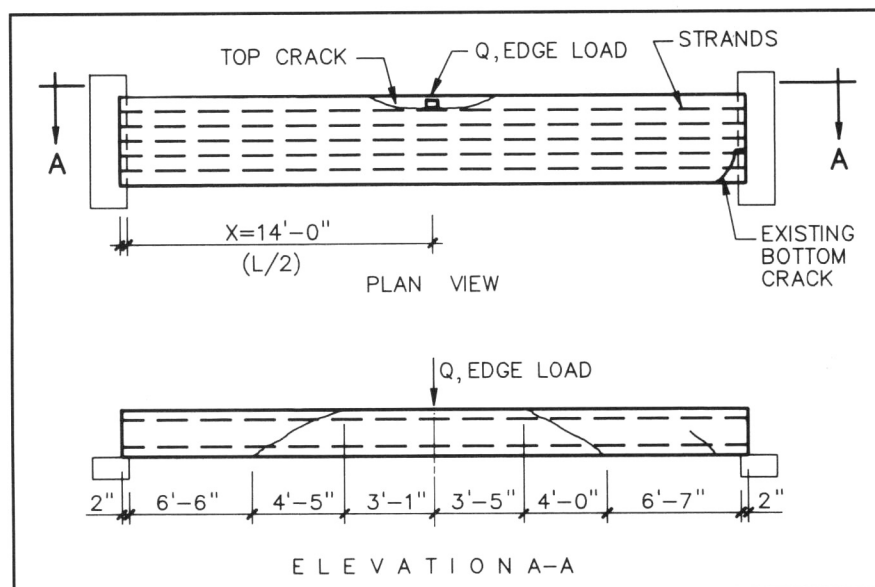


Fig. 13. Plan view and side elevation sketches showing extension of cracking.

the probabilistic approach outlined in Refs. 18 through 20. Following the procedure in Ref. 20, a pair of reasonable "safety indices" was selected where the "safety index" is the number of standard deviations away from the average which produces the desired probability of failure.

For this application, the "safety indices" are chosen equal to 3.5 for the resistance (understrength) side of the equilibrium equation and 3.5 for the load combination (overload) side of the equilibrium equation. Following the procedure outlined in Appendix A,

the allowable service load is calculated as 3.77 kips (16.8 kN).

The data have also been analyzed in a more recent alternative probabilistic approach described in Ref. 21. Here, all 25 test results were combined and approximated by a log-normal distribution using the more recent concept of reliability index, β , and accepted distribution types for dead and live loads. This resulted in an allowable load that is a function of the dead-to-live load ratio. For $\beta = 4.5$, this is given by:

$$L = (0.15 D + 1.2) \sqrt{f'_c} - D$$

where

L = maximum allowable live load (kips)

D = dead load (kips)

f'_c = concrete strength (ksi)

Use of this alternative probabilistic approach will generally permit larger edge loads.

2. Conventional Method — The second method follows a more conventional safety factor approach to structural safety in which a safety factor is applied to the lowest bound test value taken from Tables 4 through 7. This safety factor is calculated by assuming that the average load factor for dead and live loads is 1.60, and ϕ is 0.85. Then, an added factor of safety of 1.5 patterned after FIP's recommendation is imposed. This results in a combined safety factor:

$$\{1.60/(0.85)\} 1.5 = 2.80$$

3. Minimum Safety Factor Method

— The third method is again a safety factor approach. Recognizing the brittleness and sudden character of such failures, it is believed that a minimum factor of safety of 3.5 should be applied to the average of the adjusted values shown in Tables 4 through 7.

CONCLUSIONS

1. The 25 failure test loads obtained from Test Series I, II and III on 8 in. (203 mm) thick hollow-core slabs yielded valuable information with regard to the capacity of these slabs to carry edge loads. After review of the adjusted test results in Tables 4 through 7, the tests were grouped into two main categories, namely, those with edge load at midspan and those with edge load between $x = 0.15L$ and $0.38L$.

2. The adjusted results show a reasonable spread between the maximum and minimum values within each category. This spread (≤ 1.5) is comparable to, or less than, the spread from other shear or torsion tests on reinforced or prestressed concrete beams. The overall lowest and highest adjusted failure values were 10 and 15.3 kips (44.5 and 68.0 kN), respectively.

3. Two different modes of failures were identified: local punching shear and shear-torsion near the end. In both cases, failure was sudden and brittle.



Fig. 14. Shear-torsion end failure for load at the quarter point (Test No. 14).

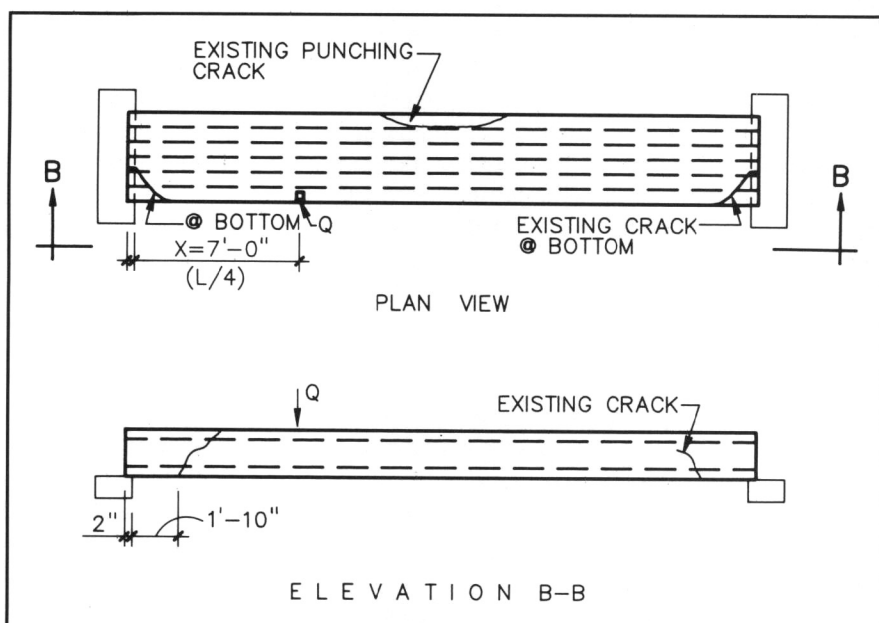


Fig. 15. Plan view and side elevation sketches showing existing crack position.

The punching shear failure involves a large three-dimensional surface centered around the edge load and flaring out 5 to 8 ft (1.52 to 2.44 m) at the lower flange level (Figs. 12 and 13). The end shear-torsion failure results in spiral-type cracking near the bearing with a diagonal crack along the vertical face of the slab (Figs. 14 and 15).

RECOMMENDATIONS

1. Following Method 1, discussed under "Service Load and Structural Safety," the maximum allowable service load is 3.77 kips (16.8 kN).

2. Following Methods 2 and 3, it is first necessary to calculate both the minimum and average test loads. For the tests listed in Table 4 (edge load at midspan), the minimum and average adjusted failure loads were 11.5 and 13.3 kips (51.1 and 59.2 kN), respectively. For Tables 5, 6 and 7 (edge load between $0.15L$ and $0.38L$), the corresponding minimum and average adjusted failure loads were 10.0 and 12.0 kips (44.5 and 53.4 kN).

3. Using these criteria and considering both a probabilistic approach and the two safety factor approaches, the following recommended maximum

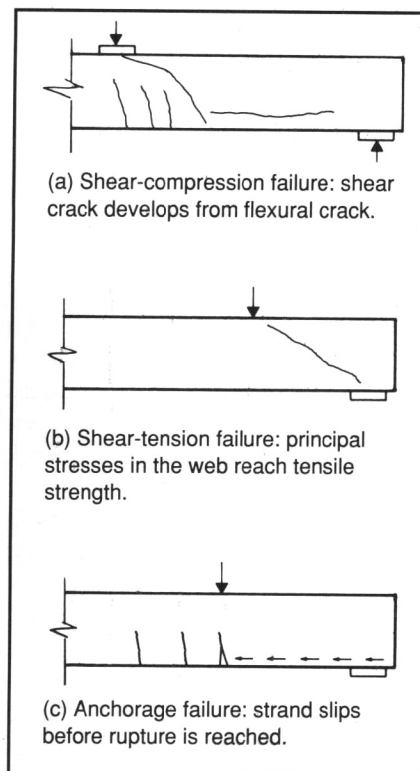


Fig. 16. Possible modes of failure when torsion is absent.

permissible service point loads as controlled either by punching shear or shear-torsion were developed.

(a) For loads at midspan, the permissible (service load) value is the lowest of:

Probabilistic approach
 = 3.77 kips (16.8 kN) (controls)
 F.S. applied to lower bound
 = $11.5/2.8$
 = 4.1 kips (18.2 kN)
 F.S. applied to average
 = $13.3/3.5$ = 3.8 kips (16.9 kN)

(b) For loads between $0.15L$ and $0.38L$, the permissible (service load) value is the lowest of:

Probabilistic approach
 = 3.77 kips (16.8 kN)
 F.S. applied to lower bound
 = $10.0/2.8$
 = 3.57 kips (15.9 kN)
 F.S. applied to average
 = $12.0/3.5$
 = 3.43 kips (15.3 kN)
 Say, 3.5 kips (15.6 kN) (controls)

For comparison, the permissible maximum edge service load based on FIP's formula, Eq. (1), for unreinforced flanges was examined.

For $f'_c = 8500$ psi and $t = 1$ in.,
 $f_c = 116 + 0.05 \times 8500$
 = 541 psi (3.73 MPa)

Therefore, the load is:

$$\begin{aligned} F &= 7.87 \times 541 \times 1/1000 \\ &= 4.26 \text{ kips (18.9 kN)} \end{aligned}$$

Note that the FIP method would suggest a slightly higher allowable load for unreinforced flanges. However, since local punching shear or shear-torsion failures control the design, this load F is superseded.

It is, therefore, recommended that the following simple conservative rules on permissible loads be adopted for geometries and prestressing levels similar to the 8 in. (203 mm) thick hollow-core slabs tested:

- If located at midspan, a maximum service load $Q = 3.8$ kips (16.9 kN) be allowed.
- If located between $0.15L$ and $0.38L$, a maximum service load $Q = 3.5$ kips (15.6 kN) be allowed.
- Linear interpolation is recommended for edge loads located between $0.38L$ and $0.5L$.

If a strictly probabilistic approach is desired, Ref. 21 should be consulted. Typically, this will yield values 10 to 14 percent higher.

The above-mentioned method assumes a concrete strength, f'_c , of at least 8500 psi (58.6 MPa), that two or more full slabs are available at each side of an opening, and that sufficient longitudinal prestressing is provided to meet flexural strength requirements. It is also assumed that the applied edge load is spread over a contact area of not less than 3×8 in. (76.2 \times 203 mm), that the section geometry of the slab is similar to the tested units, and that the edge slabs are of good quality concrete, without side tearing or cracking along the edges.

To ensure that minimum flexural strengths are met, it will be necessary for the designer to make a reasonable assessment of the effective lateral distribution of the point load. Specifically, the designer must estimate what percent of the point load is carried by the slab immediately adjacent to the opening.

Here, until more testing or research is available, the authors suggest following the guidelines:

1. PCI method (see Refs. 16 and 17).
2. FIP method (see Ref. 15).
3. Recommendations offered by existing research, noting that Refs. 12 and 13 offer specific guidelines for the distribution of vertical loads when the load is at the exterior edge of an exterior slab (Figs. 3, 4 and 5). Interior slabs may benefit from confinement of the grout key; however, further tests are needed to verify that a load increase is warranted.

NEEDED RESEARCH

In exploring the parameters followed in developing these recommendations and examining what changes in assumptions or refinement in theories would support an increase in the lower bound values derived in this report, the following research is recommended:

1. Recognizing that the choice of values for the safety factor was based on judgment and that considerable progress is being made on a unified approach to a probabilistic theory of structural safety, more work could be done in this area.

2. Since lintels (headers) are usually provided on each side of a hollow-core slab opening, it is common to have dual edge loads on one side of a slab. Therefore, additional tests using a double-slab layout should be conducted to simulate full-factored uniform loads plus two edge loads located a specified distance apart.

3. Noting that each hollow-core slab still must be designed for the total gravity load it is supporting, better and more accurate prediction of lateral load distribution is desirable. This can be done through a combination of analyses and tests.

Based on deflection measurements, it is apparent that the lateral distribution of load is quite substantial even though only two slabs were available in the combined layout. However, knowledge of deflections alone is not sufficient to estimate the moments since the latter is proportional to the

second derivative of deflection.

Also, for such unusually stiff and uncracked slabs, the typical accuracy of the measured deflections in uncontrolled environments, $\pm 1/6$ in. (± 1.6 mm), is not sufficiently precise to give a design engineer confidence in the accuracy of lateral distribution calculations. Therefore, more research is required in this area.

4. Review the most recent (1988 and later) FIP and European literature on lateral load distribution for hollow-core slabs. This will help answer three important questions:

- (a) Given a certain geometry and plan layout, what is the ratio of load that can be safely assigned to the exterior slab under both service and factored loads?

- (b) At the location of a cutout, what percentage of superimposed load is transmitted through the grouted joint to the adjacent longer slabs through the grout joint direct as compared to the load carried by the lintel (header)?

- (c) What load causes failure if it is not concentrated (e.g., a line load caused by a wall)?

ACKNOWLEDGMENTS

This investigation was carried out for the Dy-Core Manufacturers Association. Finfrack Industries, Inc., manufactured the Dy-Core slabs and all testing was conducted at its plant in Orlando, Florida. The full report on the tests was published by Dy-Core Systems Inc., Vancouver, British Columbia, Canada (see Ref. 1).

The authors would like to thank Greg Black, engineering manager for Finfrack Industries, as well as John Soucie and Bill Sanders, for their help and generous assistance in all phases of the testing program.

The authors also wish to express their sincere thanks to A. A. J. Reijgersberg in the Netherlands and to Luigi Giacomelli in Italy for furnishing and clarifying certain sections of the investigation dealing with FIP and Italian practices.

REFERENCES

1. Aswad, Alex, and Jacques, Francis J., "Test Report on Concentrated Vertical Edge Loads on Prestressed Dy-Core Slabs," Report for Dy-Core Manufacturers Association, Canada, 1989.
2. LaGue, D. J., "Load Distribution Tests on Precast Prestressed Hollow-Core Slab Construction," *PCI JOURNAL*, V. 16, No. 6, November-December 1971, pp. 10-18.
3. Johnson, T., and Ghadiali, Z., "Load Distribution Test on Precast Hollow-Core Slabs with Openings," *PCI JOURNAL*, V. 17, No. 5, September-October 1972, pp. 9-19.
4. Pfeifer, D. W., and Nelson, T. A., "Tests to Determine the Lateral Load Distribution of Vertical Loads in a Long Span Hollow-Core Floor Assembly," *PCI JOURNAL*, V. 28, No. 6, November-December 1983, pp. 42-57.
5. Beneditti, D., and Fontana, A., "Sul Comportamento Statico degli Impalcati a Panelli Prefabbricati" [On the Static Behavior of Precast Floor Panels], in Italian, *L'Industria Italiana del Cemento*, No. 12, 1975, pp. 729-734.
6. Lutrin, P., and Delvaux, C., "Resultats des Recherches sur des Elements de Plancher en Béton Précontraint pour Bâtiments" [Results of Research on Prestressed Concrete Floor Elements for Buildings], in French, *Annales de L'Institut Technique du Bâtiment et des Travaux Publics*, No. 354, October 1977, Serie Béton No. 171, pp. 54-70.
7. Computerized Structural Design, "The Behavior of a Spancrete Floor System Subjected to Non-Uniform Loads with Special Consideration of Headers and Openings," Final Report to the Spancrete Manufacturer's Association, Milwaukee, WI (undated).
8. Computerized Structural Design, "Concentrated Loads on Spancrete Assemblies," Final Report to the Spancrete Manufacturer's Association, Dr. Buettner and R. J. Becker, Milwaukee, WI, June 1980.
9. Computerized Structural Design, "Shear Considerations in Spancrete Deck Systems" (Draft), Report to the Spancrete Manufacturer's Association Technical Committee, Milwaukee, WI, March 1984.
10. Stanton, J. F., "Distribution of Vertical Load," Concrete Technology Associates, *Technical Bulletin No. 81B5*, Tacoma, WA, 1983, 102 pp.
11. Stanton, J. F., "Point Loads on Precast Floors," *ASCE Journal, Structural Engineering*, V. 109, No. 11, December 1983, pp. 2619-2637.
12. Stanton, J. F., "Distribution of Vertical Loads in Precast Concrete Decks," Final Report to PCI, Department of Civil Engineering, University of Washington, Seattle, WA, May 1988.
13. Stanton, J. F., "Response of Hollow-Core Floors to Concentrated Point and Live Loads" (to be published in May-June 1992 *PCI JOURNAL*).
14. Venkataswarlu, B., Shanmugasundaram, J., and Shanmugam, V., "Roof and Floor Slabs Associated with Precast Concrete Cored Units," *ACI Journal*, V. 79, No. 2, January-February 1982, pp. 50-55.
15. "Design Principles for Hollow-Core Slabs Regarding Shear and Transverse Load Capacity, Splitting and Quality Control," Technical Report, Fédération Internationale de la Précontrainte, Wexham Springs, Slough, United Kingdom, 1982.
16. *PCI Manual for the Design of Hollow-Core Slabs*, First Edition, Precast/Prestressed Concrete Institute, Chicago, IL, 1985.
17. *PCI Design Handbook — Precast and Prestressed Concrete*, Third Edition, Precast/Prestressed Concrete Institute, Chicago, IL, 1985.
18. Winter, George, "Safety and Serviceability Provisions in the ACI Building Code," *Concrete Design: U.S. and European Practices*, SP-59, American Concrete Institute, Detroit, MI, 1979, pp. 35-49.
19. Mirza, S., Kikuchi, D., and MacGregor, J., "Flexural Strength Reduction Factor for Bonded Prestressed Concrete Beams," *ACI Journal, Proceedings*, V. 77, No. 4, July-August 1980, pp. 237-246.
20. MacGregor, J., "Load and Resistance Factors for Concrete Design," *ACI Journal, Proceedings*, V. 80, No. 4, July-August 1983, pp. 279-287.
21. Aswad, A., and Tabsh, S. W., "Probabilistic Analysis of Hollow-Core Slabs Subjected to Edge Loads," *Concrete International*, American Concrete Institute, Detroit, MI, V. 13, No. 9, September 1991, pp. 58-63.

APPENDIX A — PROBABILISTIC APPROACH TO STRUCTURAL SAFETY

The safety indices chosen are 3.5 for the resistance (understrength) side of the equilibrium equation and 3.5 for the load combination (overload) side of the equilibrium equation. Following the discussion in Ref. 19, the value of 3.5 is selected on the high side to reflect the brittle nature of punching shear type failures.

The two safety indices can be converted to a probability of failure by standard tables and are equal to 1 in 2149. A combined probability of failure is calculated by multiplying the two probabilities and results in an overall probability of

failure of 1 in 4.6 million. This probability of failure is compatible with that historically provided for shear type failures in reinforced concrete beams (see Ref. 17). The resulting probability can then be converted back to an overall safety index of 5.62.

Table A1 shows the calculation of the average and standard deviation for the adjusted test loads. These values are used in the calculation of the allowable service load as follows:

$$\begin{aligned} \text{Allowable } Q &= \text{Average } Q - (\text{Standard deviation} \times \text{overall safety index}) \\ &= 12.36 - (1.53 \times 5.62) \\ &= 3.77 \text{ kips} \end{aligned}$$

Fig. A1 shows a plot of the test data points and the distribution check calculations.

Table A1. Statistical analysis of edge load tests on hollow-core slabs (all tests).

Location	Series	Test	Q^* (kips)	Q^2
Midspan	I	1	14.60	213.16
	I	6	14.50	210.25
	II	8	14.20	201.64
	II	10	12.60	158.76
	II	11	12.60	158.76
	II	13	11.50	132.25
0.33L to 0.38L	I	2	10.80	116.64
	I	4	-----	-----
	I	9	12.10	146.41
	I	10	12.10	146.41
	II	2	11.20	125.44
	II	3	11.20	125.44
	II	4	10.70	114.49
	II	4	10.70	114.49
0.23L to 0.25L	I	5	13.10	171.61
	II	7	13.00	169.00
	II	7	15.30	234.09
	II	12	10.00	100.00
	II	14	10.90	118.81
	III	16	13.10	171.61
	III	17	12.50	156.25
	III	17	12.50	156.25
0.15L to 0.18L	I	3	13.10	171.61
	I	7	10.00	100.00
	I	8	11.20	125.44
	II	5	11.20	125.44
	III	19	15.10	228.01
	III	20	12.50	156.25

Note: 1 kip = 4.45 kN.

* Test loads are the adjusted values from Tables 4 through 7.

$$\Sigma Q = 309.10; \Sigma(Q^2) = 3877.77$$

$$\text{Avg. } Q = 12.36 \text{ kips}$$

$$\text{Standard deviation} = \sqrt{\frac{\Sigma(Q^2) - \frac{(\Sigma Q)^2}{n}}{n - 1}} = \sqrt{\frac{3877.77 - \frac{(309.10)^2}{25}}{25 - 1}} = 1.527$$

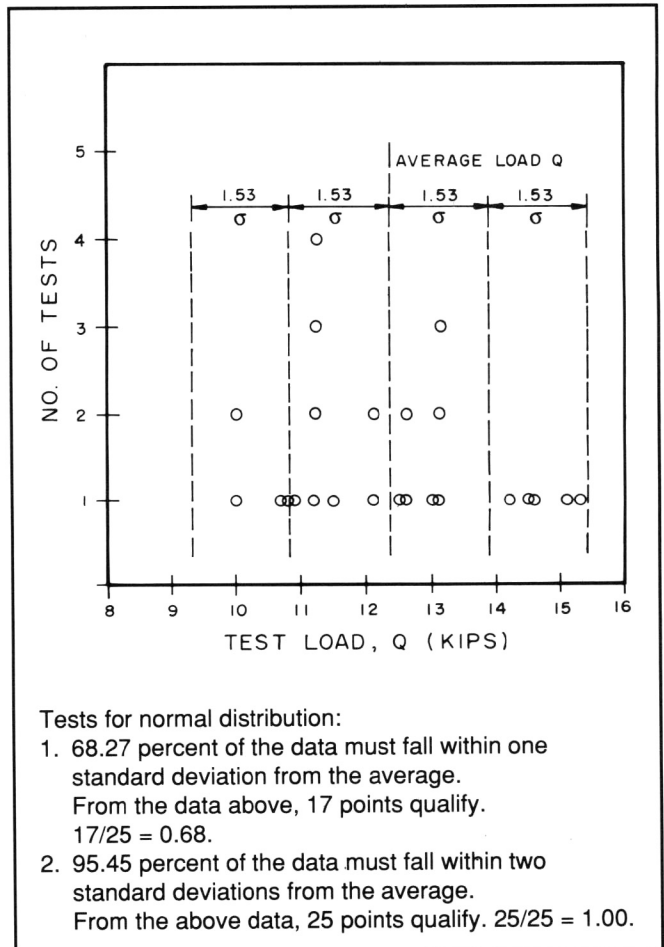


Fig. A1. Load distribution vs. number of tests.